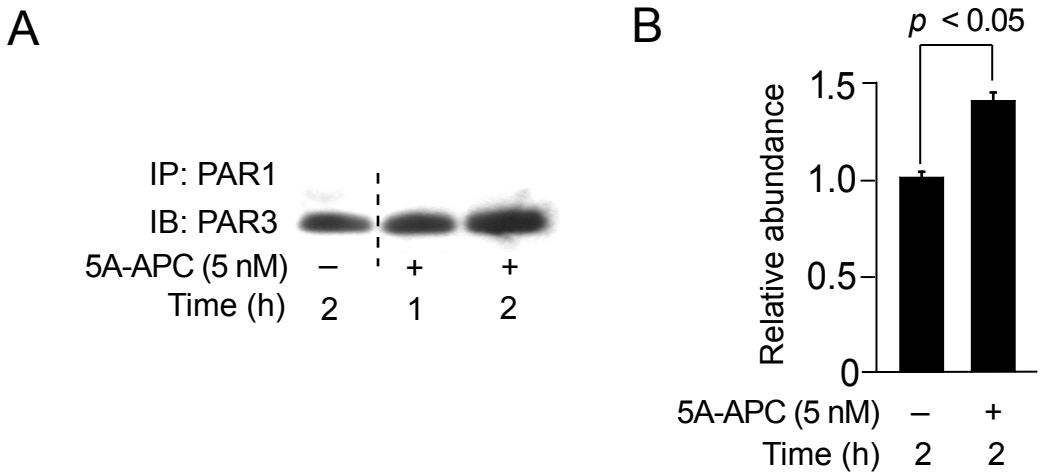

Supplementary Figure 1. (A) The cytoplasmic membrane proteins from N2a-SOD1^{G85R} cells were immunoprecipitated (IP) with the H-111 anti-PAR1 antibody, separated by 4-12% Bis-tris gel electrophoresis and immunoblotted (IB) with the M-20 anti-PAR3 antibody. The N2a cells were treated with either vehicle for 2 h or 5A-APC (5 nM) for 1 to 2 h. **(B)** The signal intensity of PAR3 bands in the presence of 5A-APC relative to vehicle was determined by quantitative densitometry. Mean ± SEM, from n=3 independent cultures.

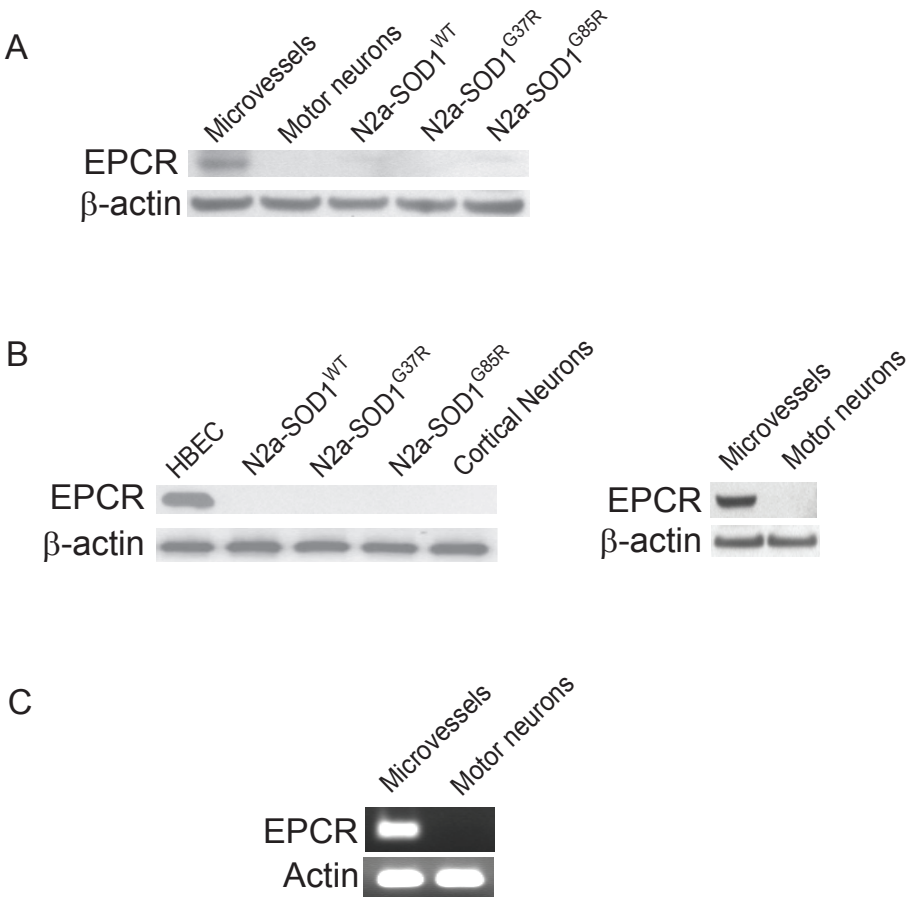

Supplementary Figure 2. (A) EPCR expression in mouse spinal cord microvessels (micorvessels, positive control) and its absence in motor neurons and mouse N2a-SOD^{WT}, N2a-SOD1^{G37R} and N2a-SOD1^{G85R} cells studied by immunoblotting with a mouse EPCR-specific antibody (RMEPCR1560). (B) EPCR expression in primary human brain endothelial cells (HBEC, positive control) and its absence in N2a-SOD^{WT}, N2a-SOD1^{G37R} and N2a-SOD1^{G85R} cells and primary mouse cortical neurons (left) studied by immunoblotting with an anti-human EPCR RCR-252 antibody (50). EPCR expression in mouse spinal cord microvessels and its absence in motor neurons (right) studied with RCR-252 antibody. (C) Semi-quantitative RT-PCR for EPCR mRNA in mouse spinal cord microvessels and motor neurons. Following primers were used; forward 5'-AGCCAAACAGGTCGCTCTTA-3' and reverse 5'-AGTCCAGCCCTTTCTCCAAG-3'.

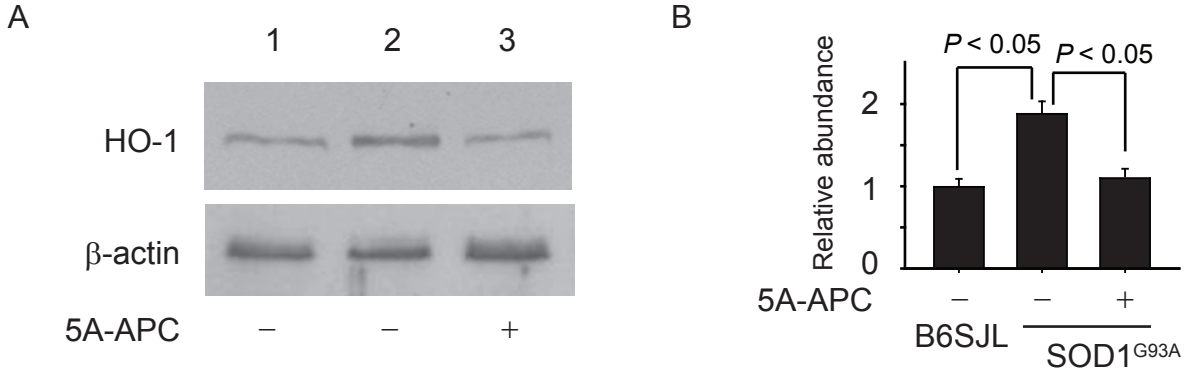

Supplementary Figure 3. (**A**) Western blot analysis of hemoxygenase 1 (HO-1) in lumbar spinal cord tissue lysates of B6SJL (lane 1) or $SOD1^{G93A}$ mice treated daily with saline (lane 2) or 5A-APC (100 μg/kg per day i.p.; lane 3) for four weeks after disease onset. (**B**) The signal intensity of HO-1 bands normalized to β-actin abundance was determined by quantitative densitometry. Mean ± SEM, n = 3 -5 mice per group.

Supplementary Methods

Mouse recombinant APC variants. There was no detectable thrombin based on thrombin time clotting assay using purified fibrinogen. This test showed no clot detected in 4000 sec, corresponding to undetectable thrombin (< 0.4 ng) per 1,200,000 ng APC in the APC preparations.

APC arterial plasma profiles. The femoral artery was cannulated with PE-50 catheter. The volume of withdrawn blood was replaced with saline containing 8 % dextran (70 kDa). Blood samples were collected in an anticoagulant solution (120 mM ethylenediaminetetraacetic acid, 300 mM benzamidine-HCl, 10 mM Hepes pH 7.5) at 9:1 ratio. Plasma was separated by centrifuging at 2,500 g for 30 min at 15° C.

APC ELISA. Briefly, the sandwich ELISA uses an anti-murine anti-protein C antibody as a capture antibody and human protein C inhibitor (PCI) as a detection reagent, taking advantage of the facts that the mouse lacks plasma PCI and that human PCI forms a 1/1 stable complex with mouse APC. The amount of complex APC:PCI is detected with an anti-human PCI monoclonal antibody.

Amidolytic assay. Purified mouse APCs were serially diluted in buffer containing 50 mM Tris, 100 mM NaCl, 0.1% BSA, pH 8. (total volume 100 µl) and placed into wells of a microplate. Then, 1.0 mM S-2366 (100 µl) was added and the rate of chromogenic substrate cleavage was determined on Optimax plate reader from Molecular Devices.

Coagulation assay. A modified Activated Partial Thromboplastin time (APTT) clotting assay that was dependent primarily on inactivation of limiting amounts of mouse factor V was performed to compare the anticoagulant activity of wt-APC and its analogs in presence of increasing concentrations of purified mouse wt-APC or APC variants (3K3A-APC, 5A-APC, S360A-APC). Human Factor V deficient plasma (Haematology TechnologiesT) containing 4 % mouse plasma as a source of factor V was incubated with the coagulation activator, Platelin LS (BioMerieux) and APC in a buffer containing 0.01 M Tris, 0.14 M NaCl, and 0.5 % bovine serum albumin, pH 7.4 for 180 sec at 37 °C and then 30 mM calcium chloride was added to initiate clotting.

^{125}I-5A-APC uptake into the lumbar spinal cord.

Radioiodination. 5A-APC (10 µg) was radiolabeled using 0.2 mCi Na^{125}I by Iodo-Gen (Thermo scientific, Rockford, IL). Free iodide was removed by gel-filtration. ^{125}I-5A-APC had a specific activity of ~ 0.5 µCi/µg. It was stored at -80^{o}C and used within 24 hr of labeling. ^{125}I-5A-APC injected to mice was > 99% trichloracetic acid (TCA) precipitable indicating no protein degradation.

Calculations. The unidirectional uptake of tracers from blood to the spinal cord ISF was determined during a linear phase of tracers accumulation in plasma (see below), as reported (19). ^{125}I-5A-APC TCA-precipitable and ^{99m}Tc-albumin TCA precipitable counts were determined using a Wallac Vizard Gamma Counter (Perkin Elmer), as described (19).

The volume of distribution of ^{125}I-5A-APC in the lumbar cord ISF, V_D (ml/g), was determined during the linear phase of tracers accumulation in plasma within first 15 min using eq. 1, as reported (59),

V_D = [(^{125}I-5A-APC TCA-precipitable c.p.m./g ISF)/(^{125}I-5A-APC TCA-precipitable c.p.m.)/ml plasma x 0.5] – [(^{99m}Tc-albumin TCA-precipitable c.p.m./g ISF)/ (^{99m}Tc-albumin TCA-precipitable c.p.m./ml plasma) x 0.5] (eq. 1)

Both ^{125}I-5A-APC and ^{99m}Tc-albumin (TCA-precipitable radioactivities) exhibited similar arterial plasma profiles with linear accumulations in plasma within first 15-20 min. This was followed by an exponential decline in their plasma levels over next 160 min. The arterial plasma concentration of ^{125}I-5A-APC in nmoles/L, C_{Pl}, was calculated from APC's specific activity. A correction factor 0.5 for the linear ramp function of tracers distribution in plasma was applied to both tracers, as reported (19).

The volume of ISF was assumed to be 0.1 ml/g of the spinal cord or about 10%, as previously reported for brain (29,59) and spinal cord (19).

The concentration of ^{125}I-5A-APC in the ISF, C_{ISF} (nmoles/l ISF) was determined from APC's V_D value at 15 min and its concentration in plasma, C_{Pl}, by using eq. 2, as reported (59),

$$C_{ISF} = V_D.C_{Pl} \qquad \text{(eq. 2)}$$

Blockade of EPCR in SOD1^{G93A} mice. Eight weeks old male SOD1^{G93A} mice were treated with either saline or 5A-APC (100 μg/kg/day i.p.) for 7 days in the absence and presence of an EPCR blocking antibody directed at an APC binding site on EPCR (RCR-252, gift from Dr. Fukudome, (41) or non-immune rat IgG (Sigma-Aldrich Inc., Saint Louis, MO). RCR-252 (40 μg/mouse) or control non-immune IgG (40 μg/mouse) were infused through the femoral vein at day 1 and 3. The dose of EPCR blocking antibodies was comparable to that used previously in mouse stroke models to block brain endothelial receptors in vivo (5). Animals were sacrificed after 7 days. The expression of human mutant SOD1 was determined at the mRNA level by QPCR analysis of laser captured motor neurons and microvessels (see below) and at the protein level by Western blotting of spinal cord motor neuron cells and spinal cord microvessels lysates (see below).

Motor neuron-enriched cell suspension. Briefly, ventral horn spinal cords were digested with 0.25% trypsin-EDTA (Gibco) at 37^{o}C for 20 min and then triturated gently using pipettes. The digested tissue was transferred to a 10 ml centrifuge tube on ice and the remaining tissue was further digested in 0.25% trypsin-EDTA for another 20 min. The total cell suspension was centrifuged at different speeds (20 x g, 50 x g, 160 x g and 1400 x g) for cell sorting. The pellets form each spin-down were either lysed with 50 μl lysis buffer (Cell Signaling Technology) for western blot analysis or spin down to a Cytoslide using Shandon CytoSpin® 3 Cytocentrifuge (Thermo Scientific) for immunohistochemical characterization. The cells attached to the cytoslide were fixed with acetone for 15 min and then blocked by 5% swine serum for 1 h at room temperature. Monoclonal mouse anti-mouse NeuN antibody (1: 500; Millipore, Billerica) and a rabbit anti-mouse polyclonal choline acetyltransferase (1:500; ChAT; Millipore) antibody, and monoclonal mouse anti-mouse GFAP antibody (1:1000; Cell Signaling Technology) were

used to characterize isolated motor neurons and contributions by astrocytes, respectively. AlexaFluro 488 donkey anti-mouse IgG (1:200, Molecular Probes) and AlexaFluro 594 donkey anti-rabbit IgG (1:200, Molecular Probes) were used as secondary antibodies. In the 50 x g fraction, 87% cells were NeuN positive. Of these NeuN positive neurons, about 90% were ChAT positive motor neurons.

Isolation of microvessels by detxran density centrifugation gradient. Briefly, mouse spinal cords from five $SOD1^{G93A}$ and B6SJL mice at 105 days of age,were homogenized in a tissue grinder with 3 strokes. A 15% dextran solution was added to homogenates for separation of microvessels by dextran density gradient centrifugation. The pellet containing microvessels was resuspended in phosphate buffered saline (PBS)/2% fetal bovine serum (FBS) and passed through 100 nm and 40 nm nylon filters in tandem to remove larger blood vessels and cell debris. The purified microvessels were prepared for different types of Western blot analysis.

N2a cultures.

Oxidant stress. Total Hb concentration was measured by QuantiChrom Hemoglobin assay Kit (Bioassay Systems). Concentrations of Oxy-Hb, Deoxy-Hb and Met-Hb in the culture medium were determined by spectrophotometric method (ref. R1) at time 0 and after 16 h. The absorbance of samples was determined at 560, 576 and 630 nm. The percentages of Oxy-Hb, Deoxy-Hb and Met-Hb species were determined by using the equations Oxy-Hb = $(1.013\ A_{576} - 0.3269\ A_{630} - 0.7353\ A_{560}) \times 10^{-4}$ M, Deoxy- Hb = $(1.373\ A_{560} - 0.747\ A_{576} - 0.737\ A_{630}) \times 10^{-4}$ M and Met-Hb = $(2.985\ A_{630} + 0.194\ A_{576} - 0.4023\ A_{560}) \times 10^{-4}$ M, as reported (ref. R1).

Oxy-Hb and deoxy-Hb have been reported to be the most toxic Hb species (Ref. R1). In the present study, Hb was a mixture of Oxy-Hb 89.4% (± 0.57%), deoxy-Hb 4.6% (± 0.13%) and Met-Hb 5.9% (± 0.12). After 16 h incubation with N2a cells, Oxy-Hb levels dropped to 76.7% (± 0.17), and deoxy-Hb and Met-Hb levels increased to 9.9% (± 0.31) and 13.3% (± 0.15), respectively [mean (± SEM), n = 6 independent experiments.

NMDA-induced apoptosis in N2a-$SOD1^{G85R}$ cells. For induction of neuronal apoptosis, N2a-$SOD1^{G85R}$ cultures were exposed for 10 min to 300 μM NMDA/5 μM glycine in Mg2+-free Hank's balanced salt solution (HBSS). Control cultures were exposed to HBSS alone. After the exposure, cultures were rinsed with HBSS, returned to the original culture medium, and incubated with or without 5A-APC for 24 h.

Inhibition of PARs. A PAR1 antibody (H-111, a polyclonal raised to residues 1-111) has been demonstrated to block thrombin's action on PAR1 (ref. R2), a finding confirmed by us (5, 7). A PAR2 antibody (a monoclonal SAM-11) was raised against residues 37-50 that comprise the activation cleavage sequence of PAR2. It has been used previously both to detect PAR2 and to block PAR2 activation (refs. R3-R5). A PAR3 antibody (H-103) is a polyclonal raised against residues 1-103 (refs. R6-R8) and neutralizes the PAR3 cleavage site. Lastly, a PAR4 specific antibody (S-20, a polyclonal N terminal region) has been used multiple times previously to block PAR4 (5,7, ref. R8, ref. R9). These antibodies also cross-react with the corresponding mouse and human PARs (4, 7, 30).

QPCR analysis of hSOD1 mRNA levels was performed in N2a-$SOD1^{G85R}$ cells treated with 5A-APC (1 nM) for 48 h in the absence or presence of cleavage site blocking PARs

antibodies (20 μg/ml) added 30 min before 5A-APC. Cell viability of N2a-SOD1^{G85R} cells was determined after 16 h treatment with X/XO as above in the absence or presence of 5A-APC (5 nM) and cleavage site blocking PARs (20 μg/ml) added 30 min before X/XO and 5A-APC.

Silencing through RNA interference. N2a cells expressing SOD1 mutants were transfected with human SOD1 shRNA and control non-effective GFP shRNA (Origene Technologies, Rockville, MD). The hSOD1 shRNA was targeted to the region containing nucleotides 320-348 of the hSOD1 coding sequence. Tranfections were performed at day 1 after differentiation using lipofectamine (Invitrogen). In a typical experiment cells were transfected with 1 μg shRNA expression plasmid DNA per 2 x 10^5 cells resulting in about 50% reductions in mutant SOD1^{G85R} and SOD1^{G37R} proteins. Transfected cells were challenged with Hb 48 h later.

To block PAR1 and PAR3 expression in N2a-SOD1^{G93A} cells we used small interfering RNA (siRNA) targeting mouse PAR1 and PAR3 with the Accell siRNA technology in which the siRNA in chemically modified to promote cellular uptake (Dharmacon E-054176-00 and E-005491-00, respectively). Accell non-targeting control siRNA (Dharmacon, D-001910-10-05) which does not degrade any known mammalian mRNA was used in control experiments. N2a cells were plated in complete medium and 24 h later transfected with 1 μM siRNA diluted in Accell siRNA delivery media (Dharmacon, B-005000-100). After 72 h transfected cells were incubated with 5A-APC (5 nM) for additional 48 h and hSOD1 mRNA levels determined by QPCR.

Immunostaining analysis for Sp1. Immunofluorescent staining was done using a rabbit anti-human Sp1 antibody which cross reacts with mouse Sp1 (1:100, Millipore) and mouse anti-human MAP2 which cross-reacts with mouse MAP2 (1:100, Millipore) followed by incubation with the respective secondary antibodies, i.e., FITC-conjugated goat anti-rabbit for Sp1 and CY3- conjugated donkey anti-mouse for MAP2. On all sections we performed simultaneously nuclear Hoechst staining (Invitrogen). Cells were scanned using a Zeiss 510 meta multi-photon/confocal microscope with a 543 nm HeNe laser to detect Cy3, a 488 nm Argon laser to detect FITC, 800 nm tuned Ti:sapphire Laser (Mai Tai Spectra Physics) to detect Hoescht. The FITC signal intensity for Sp1 relative to nuclear Hoechst signal was measured with the NIH Image J software.

Western blot analysis of Sp1. The nuclear proteins from N2a-G85R cells were extracted using the NE-PER Nuclear and Cytoplasmic Extraction Reagents (Pierce Biotechnology). We used the following primary antibodies: goat polyclonal anti-rat Sp1 antibody which cross reacts with mouse Sp1 (1:100, Santa Cruz Biotechnology) and sheep polyclonal anti-mouse histone 1 (1:500, United States Biological). Rabbit polyclonal anti-mouse phospho-Sp1 (T453; 1:500, Abcam Inc.) was used in studies on p-Sp1 in cytoplasmic lysates with β-actin as a loading control.

Western blot analysis.

After electrophoretic separation, the microvessels, cell lysates or spinal cord tissue lysates were transferred to nitrocellulose membranes. The membranes were blocked for 1 h with 5% non-fat

milk in tris-buffered saline (TBS). The membranes were washed with TBS and incubated with a horseradish peroxidase-conjugated secondary antibody for 1 h.

Microvessels. The following primary antibodies were used: rat polyclonal anti-mouse EPCR (1:100, StemCell Technologies), goat polyclonal anti-human ZO-1 which cross-reacts with mouse ZO-1 (1:250, Santa Cruz Biotechnology), mouse monoclonal anti-mouse occludin (1:50, BD Biosciences), rabbit polyclonal anti-human SOD1 which cross react with mouse SOD1 (1:1000, Assay Designs), goat polyclonal anti-human β-actin which cross reacts with mouse actin (1:1,000, Santa Cruz Biotechnology).

N2a cells lysates. We used the following primary antibodies: goat polyclonal anti-human SOD1 (1:100, Santa Cruz Biotechnology), rabbit polyclonal anti-mouse SOD1 (1:200, Chemicon) and goat polyclonal anti-human β-actin which cross reacts with mouse actin (1:1,000, Santa Cruz Biotechnology).

Spinal cord tissue lysates. Detergent insoluble SOD1 fractions were prepared from spinal cord tissue homogenates of saline-treated and 5A-APC-treated $SOD1^{G93A}$ mice as descried (ref. R10). Briefly, spinal cord tissue homogenates in the lysis buffer were mixed 1:1 in buffer A (10 mM Tris-HCl pH 8.0, 1 mM EDTA pH 8.0, 100 mM NaCl, 1% Nonidet P40), sonicated for 30 s using a microprobe sonicator (Misonix Sonicator 3000, Misonix) and centrifuged at 100,000 g for 10 min using Beckman L8-60M ultracentrifuge (Beckman Coulter, Inc.) to obtain pellet P1. P1 pellet was next dissolved in buffer B (10 mM Tris-HCl pH 8.0, 1 mM EDTA pH 8.0, 100 mM NaCl, 0.5% Nonidet P40) by sonication for 30 s following by centrifugation at 100,000 g for 10 min to obtain pellet P2. P2 pellet was mixed in buffer C (10 mM Tris-HCl pH 8.0, 1 mM EDTA pH 8.0, 100 mM NaCl, 0.5% Nonidet P40, 0.5% deoxycholic acid, 0.25% SDS), sonicated for 30 s and centrifuged at 100,000 g for 10 min to obtain pellet P3. P3 pellet was dissolved in buffer D (10 mM Tris-HCl pH 8.0, 1 mM EDTA pH 8.0, 100 mM NaCl, 0.5% Nonidet P40, 0.5% deoxycholic acid, 2% SDS) and SOD1 aggregates were detected by immunoblotting with goat polyclonal anti-human hSOD1 (Santa Cruz Biotech). Immunoblotting of whole spinal cord tissue lysates revealed that lowering the levels of SOD1 by 5A-APC also reduced both SOD1 levels and formation of covalently crosslinked, lower mobility adducts of SOD1 (not shown).

For HO-1 detection, we used spinal cord tissue homogenates in the lysis buffer and rabbit anti-mouse HO-1 polyclonal antibody (1:500; Assay Designs).

Immunoprecipitation of PAR1-PAR3 heterodimers. The N2a-$SOD1^{G85R}$ cells were treated with 5A-APC (5 nM) for 1 to 2 h. The cytoplasmic membrane fractions were prepared using the Mem-PER membrane protein extraction reagent (Thermo Fisher Scientific Inc.). Membrane samples containing 200 μg proteins in the Immunoprecipitation Kit Lysis Buffer (Roche Applied Science) were sonicated at 4°C for 30 min and centrifuged at 20,000 x g for 20 min. The supernatants were incubated for 2 h at 4°C with the H-111 anti-PAR1 antibody to immnoprecipitate PAR1 and its complexes (Santa Cruz Biotech). Protein A/G beads were added to the mixture and incubated overnight at 4°C. Immunoprecpitated proteins were analyzed by 4-12% Bis-tris gel electrophoresis. To detect the presence of PAR1-PAR3 complexes the goat polyclonal M20 mouse anti-PAR3 antibody (Santa Cruz Biotechnology) was used for immunoblotting. Donkey anti-goat HRP-conjugated secondary antibody (Santa Cruz Biotechnology) was used as a secondary antibody.

Real-time quantitative RT-PCR. The following primers were used for amplification: β -Actin, 5'-tgttaccaactgggacga-3', 5'-ggggtgttgaaggtctcaaa-3'; hSOD1, 5'-cgtggcctagcgagttatgg-3', 5'-gaaattgatgatgccctgca-3'; mSOD1, 5'-ggcccggcggatga-3', 5'-cgtcctttccagcagtcaca-3'; MCP-1, 5'-cccactcacctgctgctact-3', 5'-tctggacccattccttcttg-3'; Icam-1, 5'-gagacgcagaggaccttaaca-3' , 5'-gggcttcacacttcacagttac-3' , 5'-agctggaggtctcggaagggagc-3' .

Endothelial-specific mutant SOD1^{G37R} deletion.

Serum protein leakage. Paraform aldehyde-fixed floating sections were prepared from 7 months old SOD1^{G37R} mice (n = 4 mice per group) and Ve-Cre SOD1^{G37R} mice (n = 4 mice per group), which corresponded to the time of disease onset in both groups. Sections from age-matched non-transgenic littermate controls (n = 3 mice per group) were prepared in the same way and studied in parallel. After blockade with 5% swine serum for 1 h at room temperature sections were incubated with a Cy™3-conjugated AffinityPure donkey anti-mouse IgG antibody (1:200, Jackson Immuno Research, West Grove, PA) and Fluorescein-labeled Lycopersicon Esculentum (Tomato) Lectin (endothelial specific marker; 1:200, Vector Laboratories, Burlingame, CA) for 1 hr at room temperature. Eight to twelve nonadjacent sections were examined in each mouse. Sections of all control and experimental mice were processed in parallel. Images were taken using a Zeiss 510 meta confocal microscope. The signal intensity of mouse IgG extravascular deposits in the ventral horns was analyzed using Image J. It is of note that the IgG signal intensity determined with co-staining with the endothelial-specific lectin was comparable to that determined with co-staining with CD31 endothelial marker, as shown in a separate set of experiments.

DNA extraction from microvessels and quantitative PCR. Briefly, vessels were resuspended in 100 µl of extraction solution (0.2 mg/ml Proteinase K, 0.2% SDS and 5 mM EDTA in PBS), incubated for 4 to 5 hours at 55 degrees, DNA was precipitated with 10 µl of 3 M sodium acetate (pH 5.2), 100 µl of isopropanol and incubation for 20 minutes on ice. After washing with 70% ethanol, the DNA pellet was resuspended in 10 mM Tris, pH 7.4, 0.1 mM EDTA. For quantitative PCR, 30 ng of DNA was amplified using iQ Supermix and iCycler real time PCR machine: 1 cycle 95 ºC, 5 min; 45 cycles of 95ºC, 15 sec, 60ºC 1 min, with 100 nM of each primers and probe specific for the human SOD1 gene: hSOD1-forward, CAATGTGACTGCTGACAAAG; hSOD1-reverse, GTGCGGCCAATGATGCAAT; and hSOD1 probe, fam-CCGATGTGTCTATTGAAGATTCTG-BHQ. Primers and probe for the normalizer mouse apolipoprotein B (apoB) were: apoB-forward, CACGTGGGCTCCAGCATT; apoB-reverse, TCACCAGTCATTTCTGCCTTTG; and apoB probe, Texas Red CCAATGGTCGGGCACTGCTCAA-BHQ2. SOD1 and apoB primer/probe sets were run in the same reaction, with every reaction run in triplicates and all samples run in parallel. The entire experiment was repeated twice and results were averaged.

ROS detection. The N2a cells were washed with pre-warmed PBS and then incubated with 5 µM 5-(and-6)-carboxy-2',7'-dichlorodihydrofluorecein diacetate (carboxy-H_2DCFDA; Invitrogen, Eugene, OR) in PBS. After 60 min, the cells were returned to pre-warmed media and incubated for an additional 60 min for recovery. The fluorescent images were taken using a Zeiss Axioskop 2 confocal fluorescent microscope.

Histology and Immunohistochemistry in SOD1^{G93A} mice.

Prussian blue staining. Briefly, acetone fixed L2-L5 lumbar sections from B6SJL and $SOD1^{G93A}$ mice 15 weeks old (n = 5 mice per group) were incubated in a 5% potassium ferrocyanide and 5% hydrochloric acid solution (1:1 working solution) for 30 min. The sections were then washed with double distilled water and subsequently counterstained with nuclear fast-red. Hemosiderin shows blue, whereas the nuclei show red and the cytoplasm shows pink. Twelve nonadjacent sections (> 250 μm apart in the L2-L5 region) were examined in each mouse. The total number of spots positive for hemosiderin was determined. To access the relative abundance of Prussian blue positive deposits per section, we divided total numbers of Prussian blue positive spots by the number of studied sections.

Immunofluorescent staining of the neuromuscular junctions. Hind limb muscle sections (14 μm) from age-matched littermate controls and $SOD1^{G93A}$ mice at 15 weeks of age (n = 4 mice per group) were fixed in acetone for 5 min and blocked with 5% swine serum for 1 h at room temperature. We used FITC-labeled α-bungarotoxin to label the endplate and a goat anti-mouse vesicular acetylcholine transporter (VAChT) polyclonal antibody (1:50; Chemicon) to label axon terminals. The secondary antibody was AlexaFluor 594 donkey anti-goat IgG (1:200, Molecular Probes). Images were taken using a Zeiss Axioskop 2 confocal fluorescent microscope. All sections from control and experimental animals were processed in parallel. The neuromuscular junctions with colocalized VACht and α-bungarotoxin signals were counted as "innervated endplates" and the neuromuscular junctions only labeled with α-bungarotoxin were counted as "denervated endplates". Twelve sections from each mouse were counted (n = 4 mice per group).

Statistical analysis. The groups were coded with indicator variables and the *P* values for the score tests from the Cox regression were reported. To control for inflated type-I error rates due to multiple comparisons, we employed the false discovery rate to ensure a family-wise type I error rate of 0.05 for all such pairwise comparisons (ref. R11).

Supplementary Reference List

R1. Pluta, R.M., Afshar, J.K., Boock, R.J., and Oldfield, E.H. 1998. Temporal changes in perivascular concentrations of oxyhemoglobin, deoxyhemoglobin, and methemoglobin after subarachnoid hemorrhage. *J. Neurosurg.* **88**:557-561.

R2. Neaud, V., Duplantier, J.G., Mazzocco, C., Kisiel, W., and Rosenbaum, J. 2004. Thrombin up-regulates tissue factor pathway inhibitor-2 synthesis through a cyclooxygenase-2-dependent, epidermal growth factor receptor-independent mechanism. *J. Biol. Chem.* **279**:5200-5206.

R3. Csernok, E., Ai, M., Gross, W.L., Wicklein, D., Petersen, A., Lindner, B., Lamprecht, P., Holle, J.U., and Hellmich, B. 2006. Wegener autoantigen induces maturation of dendritic cells and licenses them for Th1 priming via the protease-activated receptor-2 pathway. *Blood* **107**:4440-4448.

R4. Dai, Y., Wang, S., Tominaga, M., Yamamoto, S., Fukuoka, T., Higashi, T., Kobayashi, K., Obata, K., Yamanaka, H., and Noguchi, K. 2007. Sensitization of TRPA1 by PAR2 contributes to the sensation of inflammatory pain. *J. Clin. Invest.***117**:1979-1987.

R5. Olianas, M.C., Dedoni, S., and Onali, P. 2007. Proteinase-activated receptors 1 and 2 in rat olfactory system: layer-specific regulation of multiple signaling pathways in the main olfactory bulb and induction of neurite retraction in olfactory sensory neurons. *Neuroscience* **146**:1289-1301.

R6. Uehara, A., Muramoto, K., Takada, H., and Sugawara, S. 2003. Neutrophil serine proteinases activate human nonepithelial cells to produce inflammatory cytokines through protease-activated receptor 2. *J. Immunol.* **170**:5690-5696.

R7. Kim, Y.V., Di Cello, F., Hillaire, C.S., and Kim, K.S. 2004. Differential Ca2+ signaling by thrombin and protease-activated receptor-1-activating peptide in human brain microvascular endothelial cells. *Am. J. Physiol Cell Physiol* **286**:C31-C42.

R8. Balcaitis, S., Xie, Y., Weinstein, J.R., Andersen, H., Hanisch, U.K., Ransom, B.R., and Moller, T. 2003. Expression of proteinase-activated receptors in mouse microglial cells. *Neuroreport* **14**:2373-2377.

R9. Pompili, E., Nori, S.L., Geloso, M.C., Guadagni, E., Corvino, V., Michetti, F., and Fumagalli, L. 2004. Trimethyltin-induced differential expression of PAR subtypes in reactive astrocytes of the rat hippocampus. *Brain Res. Mol. Brain Res.* **122**:93-98.

R10. Wang, J., Slunt, H., Gonzales, V., Fromholt, D., Coonfield, M., Copeland, N.G., Jenkins, N.A., and Borchelt, D.R. 2003. Copper-binding-site-null SOD1 causes ALS in transgenic mice: aggregates of non-native SOD1 delineate a common feature. *Hum. Mol. Genet.* **12**:2753-2764.

R11. Benjamini, Y. & Yekutieli D. 2001. The control of the false discovery rate in multiple testing under dependency. *Ann. Stat.*, 1165-1188.